Applied Energy 168 (2016) 332–339

Contents lists available at ScienceDirect

Applied Energy

journal homepage: www.elsevier.com/locate/apenergy

Bio-inspired effective and regenerable building cooling using tough hydrogels

Shuang Cui [a], Chihyung Ahn [b], Matthew C. Wingert [a], David Leung [a], Shengqiang Cai [a,b,*], Renkun Chen [a,b,*]

[a] Department of Mechanical and Aerospace Engineering, University of California, San Diego, La Jolla, CA 92093, United States
[b] Materials Science and Engineering Program, University of California, San Diego, La Jolla, CA 92093, United States

HIGHLIGHTS

- Application of tough hydrogel as regenerable 'sweating skin' for building cooling.
- Tough gel exhibits effective evaporative cooling and extraordinary cyclability.
- Charging and discharging capability of the tough gel was retained after 50 cycles.
- Tough gel cooling could lead to substantial energy saving in buildings.

ARTICLE INFO

Article history:
Received 30 July 2015
Received in revised form 19 January 2016
Accepted 21 January 2016

Keywords:
Bio-inspired
Regenerable
Tough
Building cooling
Cyclability
Energy conservation

ABSTRACT

Innovative thermal regulation technologies could provide great potential for reducing energy consumption in buildings. In this work, we report, for the first time, the application of highly stretchable and tough double network hydrogels (DN-Gels) as durable and reusable 'sweating skins' for cooling buildings. These DN-Gels demonstrate outstanding cooling performance, reducing the top roof surface temperature of wooden house models by 25–30 °C for up to 7 h after only a single water hydration charge. More importantly, compared with single network hydrogels (SN-Gels) previously studied for cooling applications, these DN-Gels exhibit extraordinary toughness and cyclability due to their interpenetrated ionically and covalently cross-linked networks, as demonstrated by constant cooling performance over more than 50 cycles. This excellent cyclability is further demonstrated by the unaltered mechanical properties and charging capability of the hydrogels after many cycles, compared to fresh ones. By coating a 100 m^2 roof of a single house with tough DN-Gels, it is estimated that the annual electricity consumption needed for air conditioning can be reduced by ~290 kW h with associated CO_2 emission reductions of 160 kg. Our results suggest that bio-inspired sweat cooling, specifically using tough DN-Gel coatings, represents a promising energy-efficient technology for cooling buildings as well as other devices and systems.

1. Introduction

In most countries, residential and commercial buildings are one of the highest energy consumption sectors. In the United States in particular, over 40% of energy consumption and greenhouse gas emissions are related to building temperature regulation [1]. Notably, building energy consumption is still increasing at a rate of 0.5–5% annually in developed countries [2] and is expected to increase even more rapidly in developing countries. Therefore, alternative building thermal regulation technologies, based on passive systems, have been extensively studied over past decade [3–5], such as night-time ventilation in moderate or cold climate [6,7], high infrared (IR) reflective coatings for reducing energy uptake [8,9], and phase change materials (PCMs) for thermal energy storage [10–12]. Nevertheless, no current passive cooling technologies used in buildings possess ideal characteristics such as high cooling efficiency under a variety of weather conditions, high durability including resistance to thermal cycling and UV irradiation, and low cost. For example, PCMs are less effective under high solar intensity fluctuations due to their low latent heat (~hundreds of kJ kg^{-1}). More efficient and durable cooling materials and systems are needed for sustainable building cooling.

In nature, plants and animals are autonomously adaptive to increases in environmental temperature through transpiration and perspiration of water, which has one of the highest latent heats among fluids. Inspired by such passive biological cooling processes,

* Corresponding authors at: Department of Mechanical and Aerospace Engineering, University of California, San Diego, La Jolla, CA 92093, United States.
E-mail addresses: shqcai@ucsd.edu (S. Cai), rkchen@ucsd.edu (R. Chen).

http://dx.doi.org/10.1016/j.apenergy.2016.01.058
0306-2619/

several self-adaptive technologies involving bio-inspired artificial skins have been reported [13–17]. One of the more promising materials is based on superabsorbent polymers, or hydrogels, which can contain more than ~90 wt% water in their fully swollen state [18,19]. These swollen hydrogels can be applied to the roofs of buildings [20], acting as artificial 'skins' to provide cooling. By applying hydrogel coatings, heat dissipation is enhanced through the evaporation of water inside the hydrogel, enabling surface temperature reductions of 10–30 °C in various objects, such as skin [21,22], handheld electronics [23–25], Li-ion battery packages [26,27], and buildings. This remarkable autonomous cooling capability makes hydrogels an attractive candidate for energy-efficient building cooling.

Importantly, hydrogels previously investigated for cooling applications have not yet demonstrated one key feature required to truly mimic biological skins: durability and reusability for repeatable cooling. Only limited regeneration capability tests have been performed on hydrogels for cooling applications [20,26,27]. The maximum cycling number demonstrated so far is about six, which is far below the amount needed for practical cooling applications. Hydrogels utilized for bio-inspired cooling so far are often brittle, as measured by low fracture energies (~10 J m^{-2}) [28], which is orders of magnitude lower than that of human skin (~1800 J m^{-2}) [29]. These poor mechanical properties (low stretchability and toughness) severely limit the scope of cooling applications for hydrogels, where reusable and regenerable cooling is important for both long-term performance and cost-effectiveness. For example, embedding hydrogels inside roofing [20] makes it unfeasible to replace the gels after only a few cycles. Furthermore, degradation and aging of hydrogels *via* UV radiation hinders outdoor applications [30–32], such as for coating windows or building facades.

In this work, we report, for the first time, the application of a highly stretchable and tough double network hydrogel (DN-Gel) [33,34] as a regenerable 'sweating skin' for cooling buildings. Compared with single network hydrogels (SN-Gels) used in previous cooling studies [20–27], DN-Gels have significantly higher fracture energy (~9000 J m^{-2}) [35], comparable to that of animal skin [29,36]. While the toughness of DN-Gels is well established, their suitability for cyclic cooling or heating has not been studied. During the cooling process, the internal morphology (e.g., porosity) could change upon swelling/deswelling cycles, or the material may degrade after exposure to heat and UV radiation. Herein, we show that DN-Gels exhibit excellent evaporative cooling performance as well as extraordinary toughness and cyclability, as demonstrated by continual cooling performance over more than 50 cycles.

2. Materials and methods

2.1. Reagents and materials

The DN-Gel monomers, alginate (AG) and acrylamide (AAm) (99+% electrophoresis grade) were purchased from FMC BioPolymer and Alfa Aesar, respectively. A crosslinker, N,N′-methylenebis (acrylamide) (MBAA) (>98.0%) and calcium sulfate dehydrate (>99%), crosslinking accelerator, N,N,N′,N′-tetramethylethylenedia mine (TEMED) (99%), and photoinitiator, ammonium persulfate (AP) (>98.0%), were purchased from Sigma–Aldrich. The SN-Gel monomers, acrylic acid (AAc) (99.5%), and photoinitiator, 2,2-dime thoxy-2-phenylacetophenone (DMPA) (99%), were purchased from Alfa Aesar and Acros, respectively. All chemicals were used as received without any purification (see Table 1).

2.2. Hydrogel preparation

To prepare DN-Gels, AG and AAm were dissolved in DI water with weight ratios of 2%, 12%, and 86% [35]. We then added 0.06 wt% MBAA, as a cross-linker to AAm, and 0.17 wt% AP, as a photoinitiator for AAm, to the solution. After degassing the solution in a vacuum chamber, we added 0.25 wt% TEMED, as a cross-linking accelerator to AAm, and 13 wt% calcium sulfate slurry, as an ionic cross-linker to AG, for homogeneous mixing using a syringe technique. The solution was poured into a plastic petri dish, cured with UV light (λ = 254 nm) for 1 h at 50 °C, and then left in a humid box for 24 h to stabilize the reaction.

For SN-Gels, a photoinitiator solution was prepared from 0.1923 g of DMPA in 10.0 mL of DMSO [37]. The solution was sonicated until all the DMPA was dissolved, then covered and kept in the dark. A pre-polymer solution contained the monomers and cross-linking agent in a pH buffer solution with a molar ratio 7:3 of AAc to AAm and a 0.128 mol% crosslink density to the total monomer. The photoinitiator solution and the pre-polymer solution were homogeneously mixed *via* sonication for 1 h. The solution was then poured into a petri dish and polymerization was initiated by exposure to a UV lamp (λ = 365 nm) at room temperature for 10 min.

2.3. Cooling performance experiments

To investigate the cooling performance and cyclability of tough DN-Gels, we conducted cooling experiments on miniaturized model houses under simulated solar irradiation (QL 1500 Series lamp) with a maximum power density of 1000 W m^{-2}. Two identical model houses made of oak wood (with thermal conductivity of 0.17 W m^{-1} K^{-1}, density of 740 kg m^{-3}, and thickness of 0.025 m), each with a roof surface area of 64 cm^2 (Fig. 1a), were built to compare the cooling effectiveness of the DN-Gels and SN-Gels. Thermocouples were attached to the top and bottom surfaces of the roof panel on both model houses to monitor the temperature rise induced by simulated solar irradiation. To directly compare cooling performance, both types of hydrogel layers were soaked in deionized (DI) water for ~8 h prior to attaching them to the model house roofs. An acrylic adhesive was used to ensure good thermal contact between the hydrogel layer and roof. A solar simulator was used to apply a normal incident irradiance of ~800 W m^{-2} to both roofs. Similar experiments were conducted to test the cyclability of the DN-Gels and SN-Gels after reducing soaking and drying time to ~5 h, and varying incident irradiance power (700 W m^{-2} and 800 W m^{-2}). The thickness of the tough DN-Gel mats synthesized here is initially 1 cm but can reversibly expand up to 2 cm in the swollen state after storing up to 90 wt% water [34,35]. We also synthesized a 0.8 cm thick SN-Gel (Poly (AAm-AAc)) according to a reported recipe [37].

Table 1
Reagents for DN-Gel and SN-Gel synthesis.

Reagent	DN-Gel	SN-Gel
Monomer	Alginate (AG)/acrylamide (AAm)	Acrylic acid (AAc)/acrylamide (AAm)
Crosslinker	N,N′-methylenebis (acrylamide) (MBAA)/calcium sulfate	N,N′-methylenebis (acrylamide) (MBAA)
Crosslinkingaccelerator	N,N,N′,N′-tetramethylethylenediamine (TEMED)	–
Photoinitiator	Ammonium persulfate (AP)	2,2-Dimethoxy-2-phenylacetophenone (DMPA)

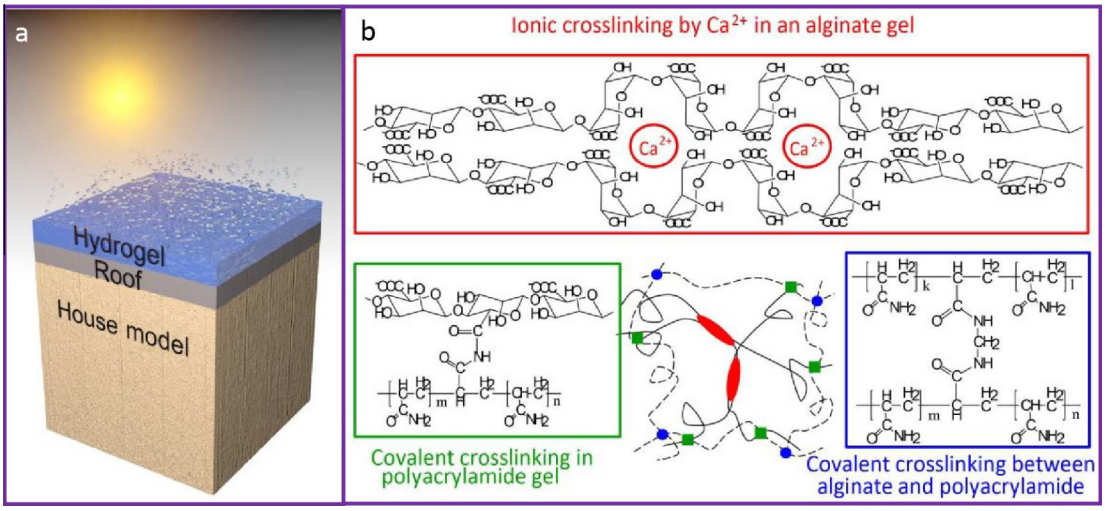

Fig. 1. (a) Schematic of the experimental setup. Miniaturized house models were covered with a hydrogel layer and subjected to simulated solar irradiation to test the effectiveness and regenerability of cooling. (b) Chemical fomula of the alginate-polyacrylamide hybrid based DN-Gel. Two types of polymer networks, ionic Ca^{2+} crosslinks (red ellipse) in the alginate gel and covalent N,N-methylenebisacrylamide (MBAA) crosslinks (green squares) in the polyacrylamide gel, intertwined and joined by covalent crosslinks (blue circles) between amine groups on the polyacrylamide chains and carboxyl groups on the alginate chains [35]. (For interpretation of the references to color in this figure legend, the reader is referred to the web version of this article.)

2.4. Mechanical property test

Dog-bone shaped specimens were laser cut according to the ASTM D-412 standard for the freshly prepared and cycled DN-Gels (after 50 cycles) in both the dehydrated and swollen states. The tensile test was conducted using an Instron 5965 universal testing instrument with a strain rate of 0.02 s^{-1}. Nominal stress was defined as the ratio between the applied force and the initial cross-sectional area of the specimen, and stretch was defined as the ratio of the current and initial length of the specimen.

2.5. Swelling ratio test

Cubes of dry gels with sides measuring 0.5 cm were immersed in DI water at a relative humidity of ~50% at room temperature. The gels were continuously retrieved from the water and, after removing excess water from the cube surface, weighed, until the gels reached fully saturated states, indicated by no additional weight gain over 3 more weighing cycles. The Swelling Ratio (SR) was defined as the ratio of the gained weight of water inside the hydrogel to that of the initial dehydrated gel [38,39].

3. Effective and regenerable cooling performance of DN-Gels

The house models covered with hydrogel layers, as shown in Fig. 1a, were built and subjected to simulated solar irradiation ranging from 700 to 800 W m^{-2}. Following Sun et al. [35] DN-Gels were synthesized, with the chemical formula of the Gel shown in Fig. 1b, which have two types of polymer networks, ionic Ca^{2+} crosslinks (red ellipse) in the alginate gel and covalent N,N-methylenebisacrylamide (MBAA) crosslinks (green squares) in the polyacrylamide gel, intertwined and joined by covalent crosslinks (blue circles) between amine groups on the polyacrylamide chains and carboxyl groups on the alginate chains [33]. For comparison, SN-Gels [37], abbreviated as poly (AAm-AAc) hereafter, were also synthesized.

3.1. Cooling effectiveness of DN-Gels

Fig. 2 shows the results of the cooling experiments on the house models coated with the DN-Gel, SN-Gel, and without any gel, which were subjected to simulated solar irradiation of 800 W m^{-2}. As shown in Fig. 2a, both types of hydrogels exhibited similar cooling capability during the first three hours of solar irradiation. In comparison to the model without an applied hydrogel coating, water evaporation from the hydrogel coated models lowered the top temperature of the roof by as much as 30 °C. However, the roof temperature of the SN-Gel coated model increased gradually after the first three hours and reached the final equilibrium temperature after four hours, which is about 30 °C and 8 °C higher than the temperature of the top and bottom surfaces of the DN-Gel coated roof, respectively. Additionally, the DN-Gel enabled a significantly longer cooling duration and continuously maintained the bottom surface of the model roof at 49 °C for up to seven hours, as shown in Fig. 2a. The longer cooling duration of the DN-Gel is also evident from the net heat flux entering the house models. The net heat input, as shown in Fig. 2b, was calculated from Fourier's law, $q = -k\frac{dT}{dx}$, where the thermal conductivity (k = 0.17 W m^{-1} K^{-1}) and thickness (0.025 m) of the roof is known and the temperature difference between the top and bottom roof surfaces was measured. Before solar irradiation, both DN-Gel and SN-Gel model houses were at room temperature. During the initial ~30 min upon solar irradiation, the temperature at the top and bottom surfaces of the house model were both increasing due to the transient heat transfer behavior (Fig. 2(a)). As a result, the net heat flux entering the house models, which was calculated based on the temperature difference between the top and bottom surfaces, also increased with time. This temperature rise resulted in higher water evaporation rate from the hydrogels, leading to decreasing net input heat flux in both the DN-Gel and SN-Gel cases from ~30 min to ~3 h. After ~3 h, the DN-Gel house reached the steady state, whereas the house covered with the SN-Gel, which contained a smaller amount of water, experienced increasing temperature and heat flux because the stored water was exhausted. With the DN-Gel layer, a much lower net heat input (~50 W m^{-2}) with constant cooling is observed compared to that of the SN-Gel layer (~250 W m^{-2}) after four hours, which shows that the DN-Gel effectively rejects about 93% of the incident solar irradiance. As we shall see later, the longer cooling duration of the DN-Gel layers is a result of the larger amount of absorbed water during the soaking period (~8 h) and a slightly larger thickness while in the dehydrated state (1.0 cm vs. 0.8 cm), compared to that of the SN-Gel.

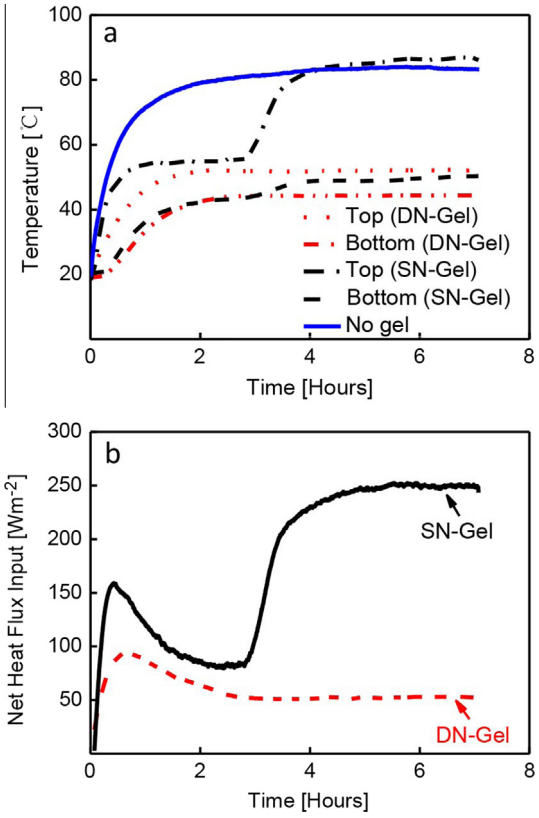

Fig. 2. (a) Comparison of the cooling effectiveness of the DN-Gel and SN-Gel. (b) Net input heat flux entering the model houses coated with DN-Gel and SN-Gel layers. The DN-Gel provides a longer cooling duration with a lower net heat flux entering the structure, compared to that of the SN-Gel.

3.2. Cooling cyclability of DN-Gels

Two model houses, each covered with a DN-Gel and SN-Gel, respectively, were subjected to repeated cycles of drying for cooling (subjected to simulated solar irradiation) and replenishing by hydration charging (soaking in water). The model house with the DN-Gel was subjected to a total of 50 cycles, with 24 cycles of 700 W m^{-2} (cloudy days) and 26 cycles of 800 W m^{-2} (sunny days) solar irradiation, at a relative humidity of ~50% (ambient temperature). The DN-Gel effectively lowered the bottom surface temperature of the house roof to 43 °C (Fig. 3a) and 49 °C (Fig. 3b) for the 700 W m^{-2} and 800 W m^{-2} solar irradiation cases, respectively. The slight variation in roof temperatures was likely caused by ambient temperature/humidity changes. The cycling experiment clearly shows that the cooling power and water storage capacity of the DN-Gel layer does not degrade after 50 cycles, demonstrating the regenerability of the cooling performance offered by the DN-Gel. As shown in Fig. 3d, after 50 cycles, the DN-Gel network still maintains integrity upon repeated volume expansion and UV irradiation, further demonstrating its durability. This degree of cyclability has not been observed in any of the previously studied artificial hydrogel skins based on SN-Gels. Furthermore, the SN-Gel layer only exhibited sustained cooling capability during the first two cycles, maintaining the bottom temperature of the roof at 43 °C (Fig. 3c) for the 700 W m^{-2} solar irradiation case. During the third cycle, the SN-Gel layer failed to cool the roof, and the bottom temperature increased to 50 °C due to collapse of the SN-Gel network (Fig. 3d).

4. Sustainable mechanical performance of DN-Gels after cycling

In order to better understand the enhanced cooling cyclability and its correlation with the mechanical properties of the DN-Gel, tensile tests on fresh and cycled DN-Gels (after the aforementioned

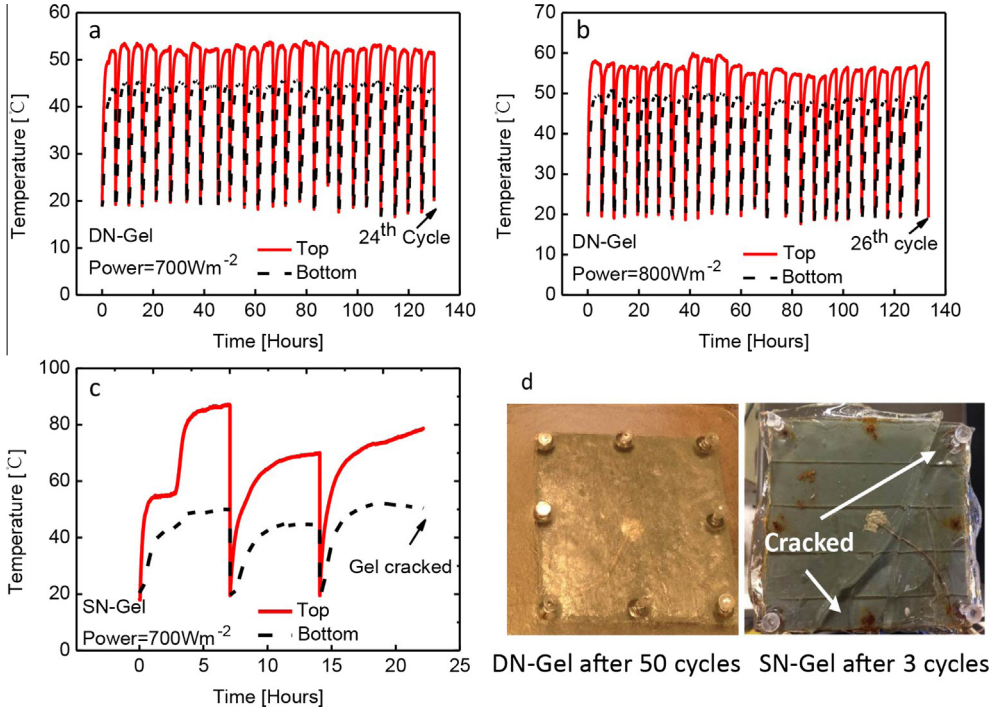

Fig. 3. Cooling cyclability test of the DN-Gel and SN-Gel. Roof temperatures for: (a) DN-Gel coating for 24 cycles (cloudy days), (b) DN-Gel coating for 26 cycles (sunny days), and (c) SN-Gel coating for 3 cycles (cloudy days). (d) DN-Gel surface (intact after the 50th cycle) and SN-Gel surface (cracked after the 3rd cycle).

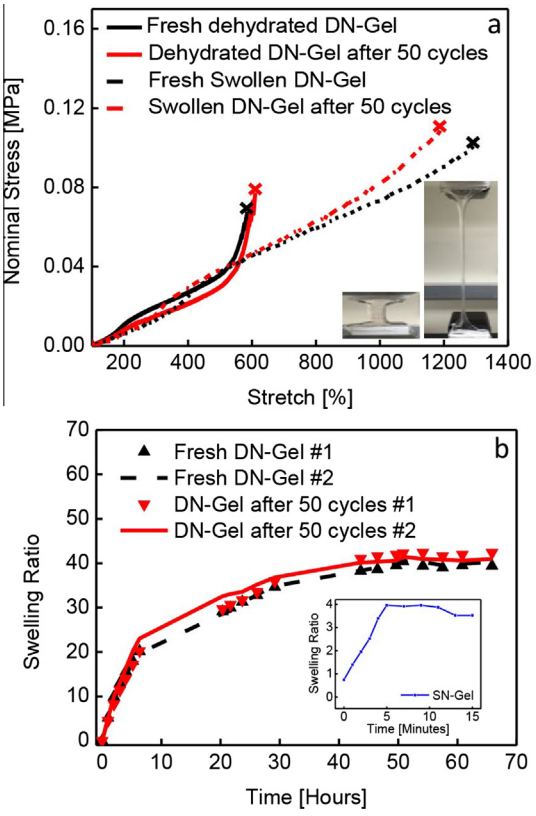

Fig. 4. (a) Sustainable mechanical properties of the DN-Gels after 50 cycles compared to fresh DN-Gels in both swollen and dehydrated states, as measured by the nominal stress vs. stretch curves. Crosses indicate mechanical breakage of the specimens. Insets are the swollen DN-Gel after 50 cycles before and during the tensile test. (b) Comparable swelling ratio (SR) of the cycled and fresh DN-Gels. Insets shows the lower SR of the specific SN-Gel studied in this work, which explains its shorter cooling duration observed in Fig. 2.

50 swelling–deswelling cycles) were performed. Fig. 4a shows that the cycled DN-Gels possess comparable stress-stretch curves to those of fresh gels, in both the swollen and dehydrated states, indicating little mechanical degradation due to cycling. The figure also shows that the DN-Gels in the dehydrated state are less stretchable than those in the fully swollen state for both fresh and cycled gels, as one would expect. The sustainable high stretchability of the swollen DN-Gel after cycling is also demonstrated by the insets in Fig. 4a for the cycled gel before and during the tensile test.

Besides the sustainable mechanical properties of the DN-Gel, the hydration (swelling) characteristics of the cycled DN-Gel layers are also comparable to the fresh ones. The cooling duration is dictated by the amount of water stored in the gel, which is characterized by the swelling ratio (SR). Fig. 4b shows the SRs of the DN-Gels as a function of soaking time, demonstrating similar swelling behavior between the cycled and fresh samples. In both types of samples, the swelling process is initially fast and gradually slows down before reaching a maximum SR of approximately 40 after 50 h. Figs. 3a, b and 4b show that the performance of the DN-Gel is not degraded during both the drying and replenishing processes, illustrating the regenerability of the hydrogels, which is important for building cooling applications.

The inset in Fig. 4b also shows that the maximum SR is only ~4 for the SN-Gel. This observation is consistent with a previous study on the SR of the same SN-Gel, namely Poly (AAm-AAc).[40] Compared to DN-Gels, the charging capacity of the SN-Gel is 4 to 5 times lower within the 8-h soaking time for the cooling effectiveness test. This explains the shorter cooling performance of the SN-Gel exhibited in Fig. 2. It should be noted that this SR behavior is specific to the SN-Gel used in this study, i.e. Poly (AAm-AAc) with an AAc : AAm ratio of 7:3, in DI water at a relative humidity of ~50% and room temperature. Other compositions of AAc and AAm of Poly (AAm-AAc) in a different PH-buffer [37,40] or other types of SN-Gels have shown larger SRs [41,42].

The fractured fresh and cycled (after 50 cycles) DN-Gels were dried via critical point drying (CPD) and the sample surfaces were examined with a scanning electron microscope (SEM). The surfaces, which fractured due to stress from the swollen state, reveal a porous structure (Fig. 5a and b) compared with those of the dehydrated DN-Gels (Fig. 5c and d). The fractured surface in the swollen state of the cycled DN-Gel (Fig. 5b) is more porous than that of the fresh one (Fig. 5a), leading to its slightly higher SR (Fig. 4b). The porous structure in the swollen state also leads to a rougher surface of the cycled specimen in the dehydrated state (Fig. 5d) after undergoing many cooling cycles. This observation is consistent with our initial hypothesis that the DN-Gels still maintain their mechanical integrity as well as the drying and replenishing performance, even after undergoing minor structural changes associated with the cycling.

5. High transparency of DN-Gel

DN-Gel coatings are advantageous over other coating materials due to their high transparency when applied on building windows. To demonstrate the effectiveness for window cooling applications, DN-Gels were placed on a transparent glass sheet under simulated solar irradiation of 800 W m^{-2}. As shown in Fig. 6a, the temperature of the glass sheet covered with the DN-Gel layer is about 10 °C lower than that of the control glass sample without a hydrogel layer over a period of 3 h. The transparency of the DN-Gels is shown in the photographs taken before and after the cooling experiments, Fig. 6b and c, respectively. Before the cooling test, the fresh DN-Gel contains over 95 wt% water. Images underneath the hydrogel layer and glass sheet are clearly visible (Fig. 6b). As the temperature increases, the DN-Gel undergoes a phase transition from a hydrated swollen state to a hydrophobic state, resulting in water release. The transparency of the DN-Gels decreases with reduced water content during cooling, as revealed by the blurry images under the DN-Gel and glass sheet in Fig. 6c. In order to adapt to different climates, the transparency of the DN-Gel can be set according to specific requirements by controlling the water content as well as evaporative cooling duration.

6. Energy and economic analysis

6.1. Energy saving performance

The heat balance on the roof surface is: $\alpha I = L_0 + h_r(T_{roof} - T_{air}) + h_c(T_{roof} - T_{air})$ [43], where α is the solar absorptance (~50% for a silver-colored roof), I is the solar insolation (maximum ~1 kW m^{-2}), L_0 is the thermal radiative cooling rate varying from 50 to 100 W m^{-2} as demonstrated in Ref. [44], h_r is the radiative heat transfer coefficient ($h_r = 4\varepsilon\sigma T_{air}^3$, $\varepsilon = 0.9$ and σ = 5.67 W m^{-2} K^{-4}), and h_c is the convective heat transfer coefficient (~6.6 W m^{-2} K^{-1}, estimated in Ref. [45] for $T_{roof} - T_{air}$ = 30 K). Therefore, the temperature difference is $T_{roof} - T_{air} = (\alpha I - L_o)/(h_r + h_c)$. Electrical energy savings and associated carbon dioxide (CO_2) emission reductions are estimated for a mid-sized house with and without the DN-Gel coating on the roof located in Southern California, shown in Table 2. In order to sustain an interior temperature of 20 °C, an air conditioner will consume ~600 kW h of electrical power per year for a house with a silver-colored roof. With a DN-Gel coating on the roof, the electricity cost and CO_2 emissions are reduced by 47% for the same house. The hydration charging of DN-Gels can be accomplished by several ways, such

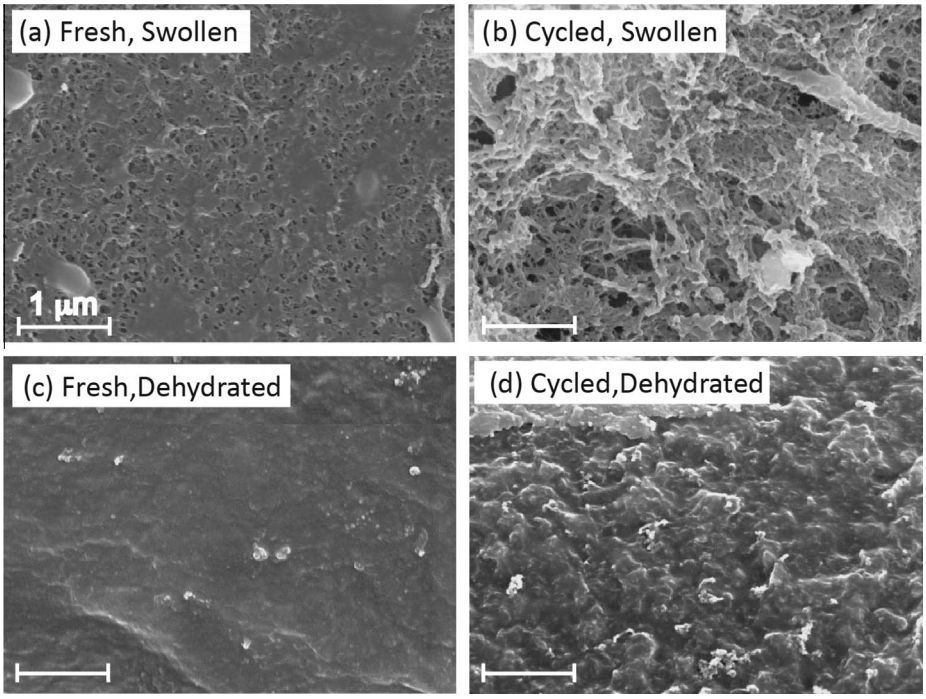

Fig. 5. Surface characteristics of the DN-Gel in the (a) fresh and (b) cycled swollen state, and (c) fresh and (d) cycled dehydrated state. DN-Gels after 50 cycles show more porous and rougher surfaces in swollen and dehydrated states, respectively. Scale bars = 1 μm.

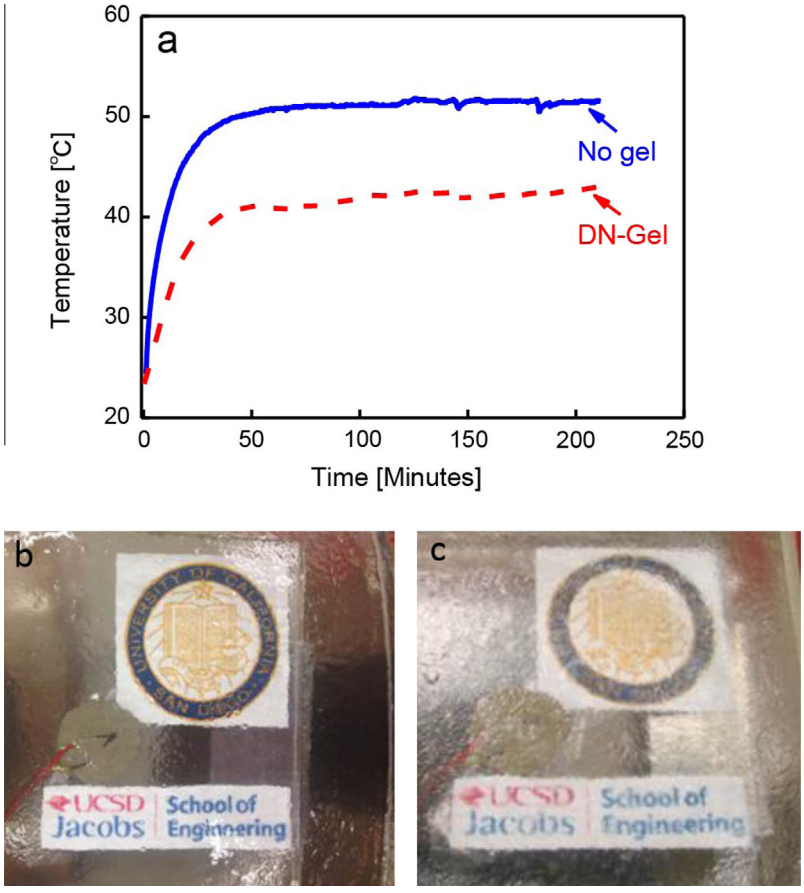

Fig. 6. (a) Cooling effectiveness of the DN-Gel on transparent glass. Transparency before (b) and after (c) cooling performance tests.

as utilizing recycled water and collecting raining water. Based on the reduction in heat uptake (31 MJ per day) and the latent heat of water, the amount of water for hydration charging is estimated to be less than 1.4 m^3 per year for a roof area of 100 m^2.

Table 2
Energy savings and CO_2 emission reduction with DN-Gel coating roof.

	$T_{outside}$ (°C)[a]	T_{inside} (°C)	Heat uptake/day (MJ)[b]	Electricity cost/year ($)[c]	CO_2 emission/year (kg)[d]
Bare roof (no gel)	67	20	~65	~90	~340
DN-Gel coating roof	45[e]	20	~34	~47	~180

[a] Calculated by assuming T_{air} = 35 °C in hot summer.
[b] Calculated as $(T_{outside} - T_{inside})UA_{house}t$ with $t = 6$ h and an overall heat transfer coefficient of roof U = 0.637 W m^{-2} K^{-1} [47]. A_{house} = 100 m^2 is the irradiated surface area.
[c] Assuming 100 hot days per year, electricity cost = $0.15/kW h, COP of an air conditioner = 3.
[d] 0.563 kg CO_2 emission per kW h [48].
[e] h_r is 4–5 times higher when hydrogel coating is applied [24].

We can further compare DN-Gel cooling technology to another emerging cooling technology, PCMs. PCMs are also a promising material for building thermal regulation but their main disadvantages are high material cost and low latent heat. For instance, paraffin, one of the most common PCMs, has a cost of $1692–1800/$m^3$ and a latent heat of 147 kJ kg^{-1} [46]. Hydrogel could be more advantageous due to its low cost ($370/$m^3$) and the associated high latent heat of water.

6.2. Manufacturing scalability and application feasibility

Tough hydrogels can be manufactured at scale with low cost. The reagents, such as acrylic acid (AAc) and its sodium or potassium salts, and acrylamide (AAm), are already being used in large volume in hydrogel manufacturing [49], e.g., baby diapers. Major equipment [50,51] involved in production, e.g. alginator and mixer, heater, and UV light for curing, are standard industrial equipment being employed in industrial polymer production [52]. Supplementary Table S1 summarizes the estimated cost of the raw materials for manufacturing tough hydrogels. The total cost is approximately $3.7 for a hydrogel sheet of 1 m^2 area and 1 cm thickness. Also, the high toughness enables the application of the DN-Gels directly on the surface for cooling with acrylic adhesive. Additionally, DN-Gels can be encapsulated in the outermost layer of roofs, windows or walls with porous covers. After evaporative cooling, the hydration charging for DN-Gels can be achieved, for instance, via automatical irrigation systems.

7. Conclusion

In summary, we have demonstrated the high cooling performance and remarkably regenerable cooling capability of tough DN-Gels for building cooling applications. The DN-Gels exhibit outstanding cooling performance by reducing the surface temperature of wood roofs and glass windows by 25–30 °C and 10–15 °C, respectively. Compared to SN-Gels, the cooling power and water absorption capacity of the DN-Gels are preserved for more than 50 cooling cycles. Compared to white roofs [53,54], hydrogels have the additional feature of high transparency [55], rendering them attractive for building window applications. Therefore, we envision that the remarkable mechanical and thermal properties of these tough DN-Gels, especially the significantly improved cyclability, will offer a novel bio-inspired energy-efficient cooling approach for buildings. Our materials could also be applied for energy-efficient thermal management of other devices and systems, such as electronics, occupational clothing, and batteries.

Acknowledgements

Acknowledgment is made to the Donors of the American Chemical Society Petroleum Research Fund for partial support of this research.

Appendix A. Supplementary material

Supplementary data associated with this article can be found, in the online version, at http://dx.doi.org/10.1016/j.apenergy.2016.01.058.

References

[1] Wang J, Zhai ZJ, Jing Y, Zhang C. Particle swarm optimization for redundant building cooling heating and power system. Appl Energy 2010;87:3668–79.
[2] Schachschal S, Adler H-J, Pich A, Wetzel S, Matura A, van Pee K-H. Encapsulation of enzymes in microgels by polymerization/cross-linking in aqueous droplets. Colloid Polym Sci 2011;289:693–8.
[3] Sadineni SB, Madala S, Boehm RF. Passive building energy savings: a review of building envelope components. Renew Sustain Energy Rev 2011;15:3617–31.
[4] Eicker U. Cooling strategies, summer comfort and energy performance of a rehabilitated passive standard office building. Appl Energy 2010;87:2031–9.
[5] Chowdhury AA, Rasul M, Khan MMK. Thermal-comfort analysis and simulation for various low-energy cooling-technologies applied to an office building in a subtropical climate. Appl Energy 2008;85:449–62.
[6] Artmann N, Manz H, Heiselberg P. Climatic potential for passive cooling of buildings by night-time ventilation in Europe. Appl Energy 2007;84:187–201.
[7] Zhou G, Yang Y, Wang X, Zhou S. Numerical analysis of effect of shape-stabilized phase change material plates in a building combined with night ventilation. Appl Energy 2009;86:52–9.
[8] Synnefa A, Santamouris M, Akbari H. Estimating the effect of using cool coatings on energy loads and thermal comfort in residential buildings in various climatic conditions. Energy Build 2007;39:1167–74.
[9] Joudi A, Svedung H, Cehlin M, Rönnelid M. Reflective coatings for interior and exterior of buildings and improving thermal performance. Appl Energy 2013;103:562–70.
[10] Zhou D, Zhao C-Y, Tian Y. Review on thermal energy storage with phase change materials (PCMs) in building applications. Appl Energy 2012;92:593–605.
[11] Soares N, Costa J, Gaspar A, Santos P. Review of passive PCM latent heat thermal energy storage systems towards buildings' energy efficiency. Energy Build 2013;59:82–103.
[12] Kuznik F, Virgone J. Experimental assessment of a phase change material for wall building use. Appl Energy 2009;86:2038–46.
[13] Liu K, Jiang L. Bio-inspired design of multiscale structures for function integration. Nano Today 2011;6:155–75.
[14] Singh AV, Rahman A, Kumar NS, Aditi A, Galluzzi M, Bovio S, et al. Bio-inspired approaches to design smart fabrics. Mater Des 2012;36:829–39.
[15] Someya T, Sekitani T, Iba S, Kato Y, Kawaguchi H, Sakurai T. A large-area, flexible pressure sensor matrix with organic field-effect transistors for artificial skin applications. Proc Natl Acad Sci USA 2004;101:9966–70.
[16] Takei K, Takahashi T, Ho JC, Ko H, Gillies AG, Leu PW, et al. Nanowire active-matrix circuitry for low-voltage macroscale artificial skin. Nat Mater 2010;9:821–6.
[17] Boucard N, Viton C, Agay D, Mari E, Roger T, Chancerelle Y, et al. The use of physical hydrogels of chitosan for skin regeneration following third-degree burns. Biomaterials 2007;28:3478–88.
[18] Gong JP, Katsuyama Y, Kurokawa T, Osada Y. Double-network hydrogels with extremely high mechanical strength. Adv Mater 2003;15:1155–8.
[19] Tanaka Y, Gong JP, Osada Y. Novel hydrogels with excellent mechanical performance. Progr Polym Sci 2005;30:1–9.
[20] Rotzetter A, Schumacher C, Bubenhofer S, Grass R, Gerber L, Zeltner M, et al. Thermoresponsive polymer induced sweating surfaces as an efficient way to passively cool buildings. Adv Mater 2012;24:5352–6.
[21] Takegami Y, Yokoyama Y, Norisugi O, Nagatsuma M, Takata K, Rehman MU, et al. Synthesis and characterization of high-quality skin-cooling sheets containing thermosensitive poly (N-isopropylacrylamid). J Biomed Mater Res Part B: Appl Biomater 2011;98:110–3.
[22] Ziemba R. The role of hydrogel dressings in prophylactic sets used by soldiers involved in polish military contingents. Burns 2013;1:2.
[23] Huang Z, Zhang X, Zhou M, Xu X, Zhang X, Hu X. Bio-inspired passive skin cooling for handheld microelectronics devices. J Electron Pack 2012;134:014501.

[24] Cui S, Hu Y, Huang Z, Ma C, Yu L, Hu X. Cooling performance of bio-mimic perspiration by temperature-sensitive hydrogel. Int J Therm Sci 2014;79:276–82.
[25] Hu Y, Zhang X, Cui S, Ren W, Yu L, Hu X. Bio-mimic transpiration cooling using temperature-sensitive hydrogel. J Chem Indust Eng 2012;63:2025–32.
[26] Zhang S, Zhao R, Liu J, Gu J. Investigation on a hydrogel based passive thermal management system for lithium ion batteries. Energy 2014;68:854–61.
[27] Zhao R, Zhang S, Gu J, Liu J, Carkner S, Lanoue E. An experimental study of lithium ion battery thermal management using flexible hydrogel films. J Power Sources 2014;255:29–36.
[28] Lake G, Thomas A. The strength of highly elastic materials. Proc R Soc Lond A: Math Phys Eng Sci: The Royal Society 1967:108–19.
[29] Qin Z, Pugno NM, Buehler MJ. Mechanics of fragmentation of crocodile skin and other thin films. Sci Reports 2014:4.
[30] Gijsman P, Meijers G, Vitarelli G. Comparison of the UV-degradation chemistry of polypropylene, polyethylene, polyamide 6 and polybutylene terephthalate. Polym Degrad Stab 1999;65:433–41.
[31] Feldman D. Polymer weathering: photo-oxidation. J Polym Environ 2002;10:163–73.
[32] Chambon S, Rivaton A, Gardette JL, Firon M, Lutsen L. Aging of a donor conjugated polymer: Photochemical studies of the degradation of poly[2-methoxy-5-(3′, 7′-dimethyloctyloxy)-1, 4-phenylenevinylene]. J Polym Sci Part A: Polym Chem 2007;45:317–31.
[33] Gong JP. Why are double network hydrogels so tough? Soft Matter 2010;6:2583–90.
[34] Gong JP. Materials both tough and soft. Science 2014;344:161–2.
[35] Sun J-Y, Zhao X, Illeperuma WR, Chaudhuri O, Oh KH, Mooney DJ, et al. Highly stretchable and tough hydrogels. Nature 2012;489:133–6.
[36] Yang W, Sherman VR, Gludovatz B, Schaible E, Stewart P, Ritchie RO, et al. On the tear resistance of skin. Nat Commun 2015:6.
[37] Fiumefreddo A, Utz M. Bulk streaming potential in poly (acrylic acid)/poly (acrylamide) hydrogels. Macromolecules 2010;43:5814–9.
[38] Yanfeng C, Min Y. Swelling kinetics and stimuli-responsiveness of poly (DMAEMA) hydrogels prepared by UV-irradiation. Radiat Phys Chem 2001;61:65–8.
[39] Kim SJ, Park SJ, Kim SI. Swelling behavior of interpenetrating polymer network hydrogels composed of poly (vinyl alcohol) and chitosan. React Funct Polym 2003;55:53–9.
[40] Duran S, Şolpan D, Güven O. Synthesis and characterization of acrylamide–acrylic acid hydrogels and adsorption of some textile dyes. Nucl Instrum Meth Phys Res Sect B: Beam Interact Mater Atoms 1999;151:196–9.
[41] Gupta NV, Shivakumar H. Investigation of swelling behavior and mechanical properties of a pH-sensitive superporous hydrogel composite. Iran J Pharm Res: IJPR 2012;11:481.
[42] Xia L-W, Xie R, Ju X-J, Wang W, Chen Q, Chu L-Y. Nano-structured smart hydrogels with rapid response and high elasticity. Nat Commun 2013:4.
[43] Berdahl P, Bretz SE. Preliminary survey of the solar reflectance of cool roofing materials. Energy Build 1997;25:149–58.
[44] Martin M, Berdahl P. Summary of results from the spectral and angular sky radiation measurement program. Solar Energy 1984;33:241–52.
[45] Kreith F, Manglik R, Bohn M. Principles of heat transfer: cengage learning; 2010.
[46] Kosny J, Shukla N, Fallahi A. Cost analysis of simple phase change material-enhanced building envelopes in southern US climates. US Department of Energy; 2013.
[47] Aktacir MA, Büyükalaca O, Yılmaz T. A case study for influence of building thermal insulation on cooling load and air-conditioning system in the hot and humid regions. Appl Energy 2010;87:599–607.
[48] Levinson R, Akbari H, Reilly JC. Cooler tile-roofed buildings with near-infrared-reflective non-white coatings. Build Environ 2007;42:2591–605.
[49] Ahmed EM. Hydrogel: preparation, characterization, and applications. J Adv Res 2013.
[50] Özkan L, Kothare MV, Georgakis C. Control of a solution copolymerization reactor using multi-model predictive control. Chem Eng Sci 2003;58:1207–21.
[51] Park M-J, Hur S-M, Rhee H-K. Online estimation and control of polymer quality in a copolymerization reactor. AIChE J 2002;48:1013–21.
[52] Alaei J, Boroojerdi SH, Rabiei Z. Application of hydrogels in drying operation. Petrol Coal 2005;47:32–7.
[53] Gaffin S, Rosenzweig C, Parshall L, Beattie D, Berghage R, O'Keeffe G, et al. Energy balance modeling applied to a comparison of white and green roof cooling efficiency. Green Roofs in the New York Metropolitan Region Research Report; 2010. p. 7.
[54] Hildebrandt EW, Bos W, Moore R. Assessing the impacts of white roofs on building energy loads. ASHRAE Trans 1998;104:810.
[55] Wang M, Gao Y, Cao C, Chen K, Wen Y, Fang D, et al. Binary solvent colloids of thermosensitive poly (n-isopropylacrylamide) microgel for smart windows. Indust Eng Chem Res 2014;53:18462–72.